Fuel 143 (2015) 577–585

Contents lists available at ScienceDirect

Fuel

journal homepage: www.elsevier.com/locate/fuel

Kinetics based on two-stage scheme for co-combustion of herbaceous biomass and bituminous coal

Xiang Liu, Meiqian Chen *, Yuanhang Wei

School of Mechanical, Electronic and Control Engineering, Beijing Jiaotong University, Beijing 100044, China

HIGHLIGHTS

- The co-combustion kinetics of beet/bituminous coal was studied.
- The co-combustion kinetics of switchgrass/bituminous coal was studied.
- The dominant mechanisms of co-combustion at pre-peak and post-peak were determined.
- There were kinetic compensation effects for selected samples within wide heating rates.

ARTICLE INFO

Article history:
Received 27 July 2014
Received in revised form 24 November 2014
Accepted 25 November 2014
Available online 11 December 2014

Keywords:
Co-combustion
Biomass
Chinese bituminous coal
Heating rate
Kinetics

ABSTRACT

The kinetics of co-combustion of two herbaceous biomass species (beetroot and switchgrass) with bituminous coal was evaluated using a non-isothermal thermogravimetric method (TGA). The effects of heating rates, sample kinds and blend ratios on the kinetics of co-combustion were revealed based on two-stage scheme, which referred to the two stages before and after the maximum combustion rate. The kinetic parameters and combustion reaction mechanisms were tested by combining the isoconversional method (Ozawa–Flynn–Wall) and the Coats–Redfern method in order to find out the kinetics characteristics responsible for the combustion of the samples. There were significant difference between combustion kinetics of bituminous coal and biomass. The blending ratios and the heating rates had have certain effect on the mechanisms of switchgrass/coal blends at pre-peak. The dominant mechanisms associated with co-combustion kinetics for beetroot/coal at pre-peak and post-peak were described by the Avrami–Erofeev equations. The mechanisms of co-combustion for switchgrass/coal samples at pre-peak were described by the Avrami–Erofeev equation, Z–L–T equation or Anti-Jander equation; however, at post-peak, their mechanisms were described by the Avrami–Erofeev equation. The general kinetic compensation effect correlations were deduced for all samples within the heating rates of 10–90 °C/min.

© 2014 Elsevier Ltd. All rights reserved.

1. Introduction

Biomass is a renewable energy source that will provide environmental and economic benefits, and biomass residues are readily available in large quantities [1]. A wide variety of biomass materials, including herbaceous and woody materials, agricultural residues and energy crops are used [2]. Switchgrass, a perennial warm-season bunchgrass native to North America, where it occurs naturally from Canada southwards into the United States and Mexico, has also been identified as having potential as an energy crop for Eastern Canada and for the US [3] . It is desirable as a potential biofuel in direct combustion systems because of its excellent burn quality, ease of management, and high yield [4]. Beetroot residue is a by-product from beet sugar production, and it is abundant especially in the US, but they are currently used for lower-value products [5]. Burning biomass alone cannot give very high energy output compared with coal combustion because of its high volatile matter and moisture content [6–8]. Co-combustion of biomass and coal in existing power plants is a most promising option for application with renewable fuels [9,10]. Muthuraman et al. detect that reactivity of coal had been improved upon blending with wood [11]. Kinetics of co-combustion of coal and pine sawdust blends have also been studied [12], the results reveal that the first step of biomass oxidation and coal combustion is effectively described by first order reaction mechanisms, and the second step of biomass combustion is more influenced by diffusion mechanisms. Kinetics of coal, palm shell and their blends are determined using the Doyle's and

---

* Corresponding author. Tel.: +86 10 51683423.
E-mail address: mqchen@bjtu.edu.cn (M. Chen).

http://dx.doi.org/10.1016/j.fuel.2014.11.085
0016-2361/© 2014 Elsevier Ltd. All rights reserved.

Nomenclature

a	degree of conversion
A	the pre-exponential or frequency factor (s^{-1})
dm/dt	burning rate ($mg\ min^{-1}$)
E_a	apparent activation energy ($J\ mol^{-1}$)
M	mass fraction of sample
R	the universal gas constant (J/(mol K))
t	temperature (°C)
T	temperature (K)

Greek letter

β	heating rate (°C min^{-1}/°C s^{-1})

Subscripts and superscripts

0	initial
∞	burning-out

Coats–Redfern's models and activation energy is found to decrease with increasing palm shell composition in coal; however, a reverse trend is observed for the pre-exponential factor.

While most of these studies about combustion of biomass and coal are conducted under a certain heating rate and usually selected biomasses mainly include wheat straw [13], corn straw and sawdust. Furthermore, kinetics analyses associated with the combustion are mainly focused on a certain stage and normally on individual biomass or coal [14–16]. The use of bituminous coal with herbaceous biomass briquettes such as beetroot and switchgrass, and assessment about the effect of various parameters, like blending ratio and heating rate with wide scope, on co-combustion kinetics are still scarce. Little information is available to date on the kinetics model of co-combustion of biomass and coal based on two-stage scheme. This paper presents kinetics on co-combustion of bituminous coal and herbaceous biomass (beetroot and switchgrass) for a wide range of blending ratios and heating rates. The main purpose of the current study is to explore the effect of heating rates, sample kinds, and biomass ratios on co-combustion kinetics based on two-stage scheme. Isoconversional and model-fitting methods for estimating kinetic parameters are comparatively evaluated. The Arrhenius parameters are analyzed to assess if there are any compensating effects.

2. Methods

2.1. Experimental facility and test samples

A thermogravimetric analyzer (TGA/SDTA851, Mettler Toledo) with a precision of 0.001 mg was used to conduct the co-combustion experiments. The beetroot and switchgrass residues were provided by University of Oakland, and Chinese pulverized bituminous coal were selected. The mixtures were obtained from a platinum crucible in which the beetroot/bituminous coal and switchgrass/bituminous coal blends were homogenized with biomass weight percentages of 20, 40, 60 and 80 wt.% by using a 180 μm sieve to sieve the samples. Prior to thermogravimetric tests, biomass and coal were well-mixed mechanically and pre-dried for 10 h at 373 K. The kinetic characteristics of the overall process are determined by the velocity of advance of this interface into the unchanged reactant and the variation in its effective area with time. Ideally, kinetic studies would be concerned with single crystals of simple and constant geometry but, in practice, it is often necessary to use assemblages of crystallites which usually contain a range of sizes. No unifying theoretical concepts have been recognized which can be used to provide satisfactory criteria for the comprehensive classification of the kinetics and mechanisms of reactions involving solids [17]. The rate determining step in any solid phase reaction can be either (i) diffusion, i.e. the transportation of participants to, or from, a zone of preferred reaction, or (ii) a chemical reaction, i.e. one or more bond redistribution steps, generally occurring at a reaction interface. In mechanistic studies, measurements are frequently concerned with rate processes from which the effects of diffusion are specifically excluded. The initial mass of each sample was maintained at 10 mg ± 0.5 mg. The detailed method had been published from my previous work in the Refs. [18,19]. The proximate analysis and ultimate analysis of the parent samples were listed in Table 1. The combustion processes were performed with heating rates of 10, 30, 50, 70 and 90 °C/min, respectively. To ensure reproducibility, the experiments were repeated three times. The results indicate that a good

Table 2
Uncertainties of the measured parameters and calculated parameters.

Parameters	Uncertainty (%)
Temperature	±0.01
Mass	±0.003
Apparent activation energy	±0.01
Pre-exponential factor	±0.014

Table 1
Proximate and ultimate analysis of samples.

Samples	Proximate analysis (wt.%)				Ultimate analysis (wt.%)					HHV (MJ/kg)
	M_{ad}	V_{ad}	A_{ad}	FC_{ad}	C_{ar}	H_{ar}	O_{ar}	N_{ar}	S_{ar}	
Beetroot	9.37	71.88	2.30	16.45	40.75	5.92	45.73	1.31	0.19	17.01
80B20C[a]	6.77	67.63	8.95	16.65						16.36
60B40C	6.57	66.14	8.96	18.33						16.72
40B60C	6.49	51.35	13.99	28.17						17.86
20B80C	4.89	50.10	14.47	30.54						18.50
Bituminous coal	2.72	22.42	29.16	45.70	68.42	3.91	1.32	12.69	0.70	19.43
Switchgrass	7.58	76.25	3.20	12.97	42.04	4.97	35.44	0.77	0.18	16.45
80S20C[b]	6.30	71.70	9.00	13.00						15.70
60S40C	5.99	68.13	12.39	13.49						15.29
40S60C	5.60	50.29	18.71	25.40						16.68
20S80C	5.49	49.80	19.58	25.13						16.50

[a] 80B20C refers to 80% beetroot/20% coal blend.

[b] 80S20C refers to 80% switchgrass/20% coal blend.

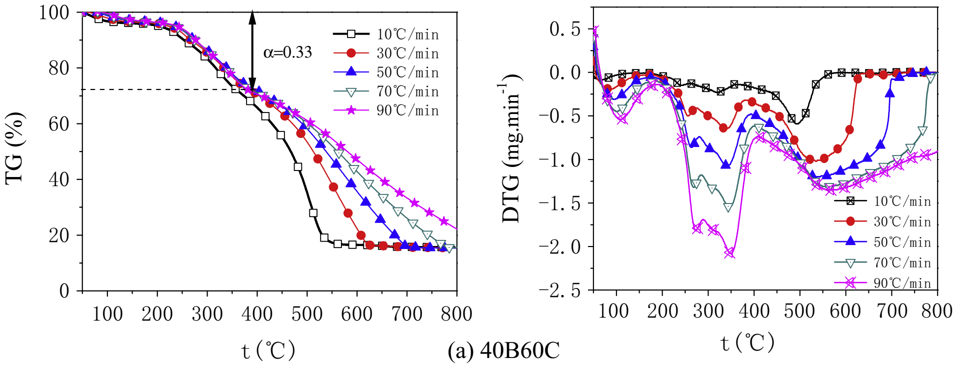

(a) 40B60C

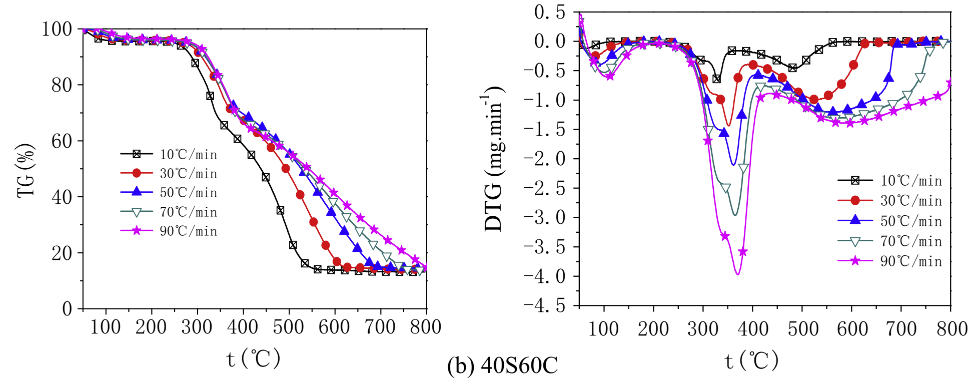

(b) 40S60C

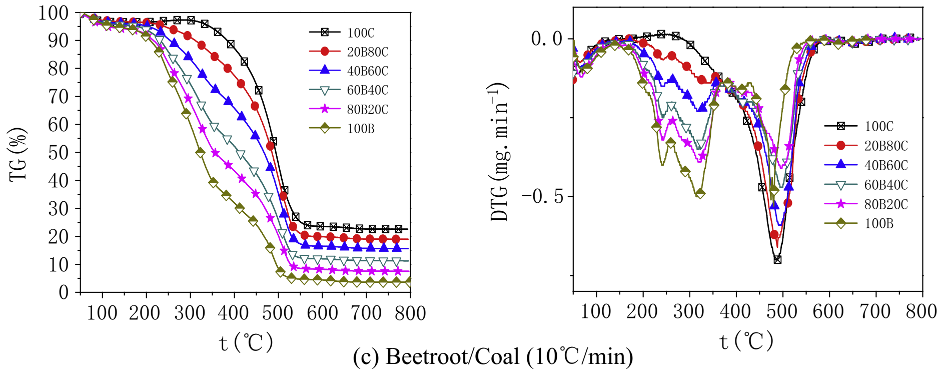

(c) Beetroot/Coal (10℃/min)

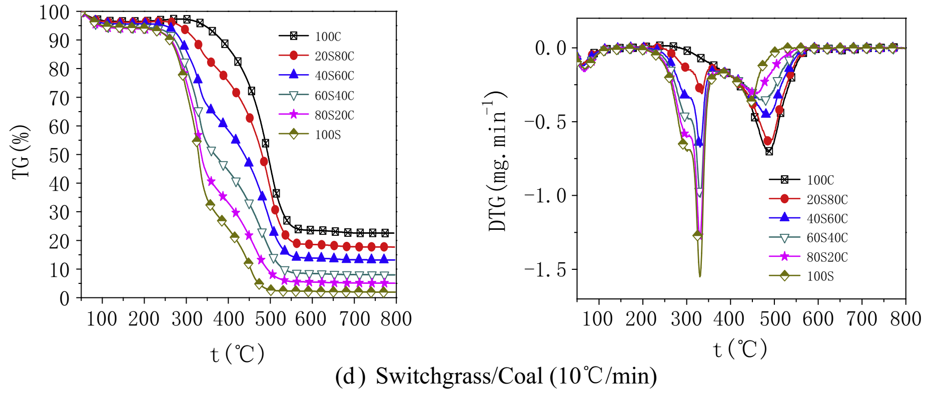

(d) Switchgrass/Coal (10℃/min)

Fig. 1. TG and DTG curves of beetroot/coal and switchgrass/coal.

reproducibility is maintained for each run because the relative deviation was generally within ±1.0%.

The uncertainties of the measurement in the experiment are dependent on the experimental conditions and the measurement instruments. Therefore, the uncertainties of independent parameters are firstly computed, and consequently uncertainties of dependent parameters are calculated based on their relationship with independent parameters described in the Section 2.2. The uncertainties of the parameters in Table 2 were estimated by using the method in Refs. [20–22].

2.2. Kinetic analysis

In order to calculate the kinetics much accurately, the main combustion region may be divided into two stages of pre-peak and post-peak by the maximum point in DTG. The reference value of activation energy of fuel around peak is calculated using the Ozawa–Flynn–Wall equation [23–28], which can be expressed as follows:

$$\log\beta = \log\left[\frac{AE_a}{RG(a)}\right] - 2.315 - 0.457\frac{E_a}{RT} \tag{1}$$

where $G(a)$ is integral representation of the mechanism function, β the heating rate (°C/min), T the absolute temperature (K) , A the pre-exponential or frequency factor (s^{-1}), E_a the activation energy (J/mol), and R the universal gas constant [J/(mol K)], a the degree of conversion at time t and it can be calculated by the following equation

$$a = \frac{m_0 - m}{m_0 - m_\infty} \tag{2}$$

where m is the weight of samples at any time, m_0 the initial weight of samples, and m_∞ the weight of samples at the end of the burning process, respectively. By the way, the mass fraction of samples, longitudinal coordinate in TG curves can be expressed as

$$M = \frac{m}{m_0} \tag{3}$$

By plotting log (β) vs. $1/T$, initial E_a can be related to certain degree of conversion.

The integral method based on the Coats and Redfern (CR) equation [29–31] is a popular non-isothermal model-fitting method that requires an assumption be made regarding formula of the mechanism function $g(a)$, which is expressed as follows:

$$\ln\left[g(\alpha)/T^2\right] = \ln(AR/\beta E_a) - E_a/RT \tag{4}$$

By substituting common solid reaction mechanism functions into Eq. (4) respectively [32], and plotting $\ln\left[g(a)/T^2\right]$ vs. $1/T$, E_a and A of fuel in each stage can be obtained. The mechanism function will be selected solely by comparing the E_a values with reference value obtained from the Ozawa–Flynn–Wall equation.

3. Results and discussion

3.1. TG and DTG curves

Although the TG and DTG curves of samples for a wide range of heating rates and blending ratios are obtained, for brevity, only some of the results are discussed. Fig. 1 illustrates the TG and DTG curves of 40B60C and 40S60C at different heating rates and all samples at heating rate of 10 °C/min.

From Fig. 1, as heating rate increases, TG profiles shift to higher temperatures, and the rate of weight loss increases, which is indicative of the advance in combustion and complete combustion at lower temperatures. The mean combustion rate, and the maximum combustion rate of samples which mainly occurs at the volatile matter combustion region, increase with increasing the heating rate, as heightening of mass transfer results from the enhancement of heat transfer. As biomass blending ratio increases, TG profiles shift to lower temperatures, and the maximum combustion rate of samples which increases due to more volatile matter in biomass, while the combustion rate which occurs at fixed carbon combustion region decreases due to less fixed carbon in biomass. After the moisture release peak, pure beetroot and beetroot/coal blends showed 3–4 peaks for combustion of volatiles and fixed carbon, reflecting the existence of complex volatiles compositions for beetroot [18]. The main combustion stages of beetroot, switchgrass and their blends with coal mainly focus at temperature range of 200–400 °C due to beetroot and switchgrass being two typical herbaceous plants which are composed of more hemi-cellulose and cellulose. The biomass is mainly composed of hemi-cellulose, cellulose and lignin, which decompose at the temperature range of 225–325, 305–375 and 250–500 °C, respectively [33].

3.2. Kinetic parameters

Fig. 1 reveals that there is a maximum value (DTG) at the temperature of 320 °C for 40% beetroot/60%bituminous coal blend at heating rate of 10 °C/min. The linear fitting is shown in Fig. 2 by plotting log (β) vs. $1/T$ for the blend ($a = 0.33$). R and SD are the correlation coefficient and the standard deviation of linear fitting, respectively [34,35]. The reference value of activation energy of the blend is obtained, 143.50 kJ/mol. The temperature range at pre-peak can be taken from 260 to 320 °C. Based on Eq. (4), by plotting $\ln\left[g(a)/T^2\right]$ vs. $1/T$ as shown in Fig. 3, the dominant mechanism is fitted to the Avrami–Erofeev equation, $G(\alpha) = [-\ln(1-a)]^4$, which is controlled by the random nucleation and then growing process. Nucleation is the process by which the reaction interface is initially established [17], at perhaps a limited number of points

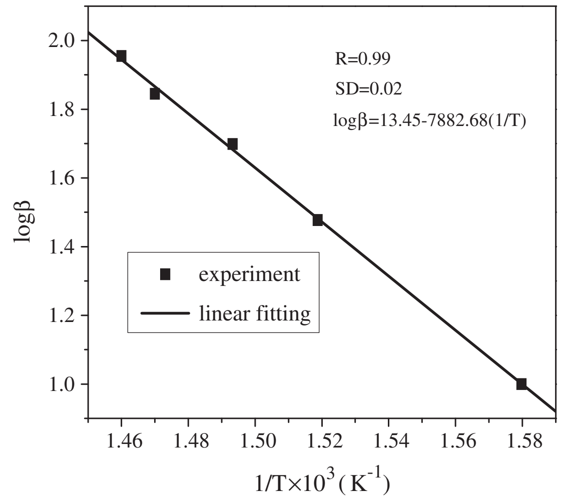

Fig. 2. Linear fitting of 40B60C by Flynn–Wall–Ozawa method.

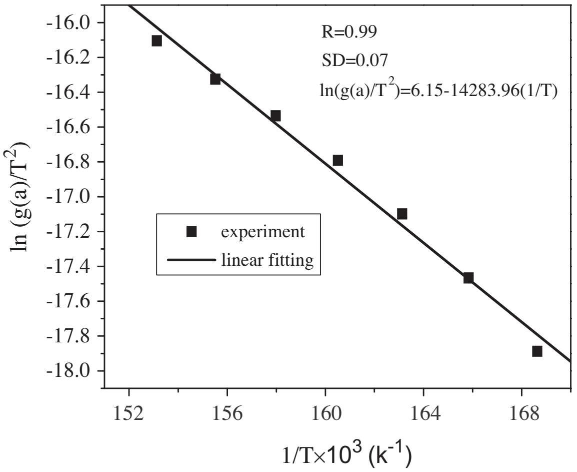

Fig. 3. Linear fitting of 40B60C at pre-peak by Coats–Redfern method at heating rate of 10 °C/min.

Table 3
Combustion kinetic parameters of beetroot/bituminous coal at pre-peak.

Samples	β (°C/min)	t (°C)	A (s^{-1})	E_a (kJ/mol)	R	SD	$g(\alpha)$
Bituminous coal	10	420.00–480.00	1.64E+02	53.63	−0.99	0.01	$\left[1-(1-a)^{0.8}\right]/0.8$
	30	465.00–515.00	3.45E+01	48.38	−0.99	0.01	$\left[1-(1-a)^{0.8}\right]/0.8$
	50	496.00–546.00	1.17E+01	43.80	−0.99	0.01	$\left[1-(1-a)^{0.5}\right]/0.5$
	70	496.00–546.00	4.25E+01	51.28	−0.99	0.01	$-\left[1-(1-a)^{0.8}\right]/0.5$
	90	524.00–574.00	7.00E+00	41.54	−0.99	0.01	$-\ln(1-a)$
20B80C	10	280.00–340.00	2.47E+05	123.96	−0.99	0.05	$[-\ln(1-a)]^4$
	30	290.00–350.00	3.94E+03	100.53	−0.99	0.03	
	50	290.00–350.00	1.24E+04	105.97	−0.99	0.02	
	70	290.00–350.00	8.27E+03	105.86	−0.99	0.01	
	90	280.00–340.00	4.79E+04	105.92	−0.99	0.03	
40B60C	10	260.00–320.00	1.12E+06	118.76	−0.99	0.04	
	30	280.00–340.00	7.95E+05	114.85	−0.99	0.01	
	50	280.00–340.00	3.13E+06	120.04	−0.99	0.01	
	70	290.00–350.00	2.93E+06	117.50	−0.99	0.02	
	90	290.00–350.00	3.95E+07	126.72	−0.98	0.03	
60B40C	10	260.00–320.00	1.01E+08	142.53	−0.99	0.01	
	30	280.00–340.00	3.63E+08	149.27	−0.99	0.01	
	50	280.00–340.00	1.37E+08	156.73	−0.99	0.02	
	70	290.00–350.00	9.13E+07	158.97	−0.99	0.02	
	90	280.00–340.00	2.67E+08	162.61	−0.99	0.04	
80B20C	10	260.00–320.00	4.18E+11	162.31	−0.99	0.09	$[-\ln(1-a)]^3$
	30	240.00–300.00	8.75E+13	181.01	−0.99	0.05	
	50	260.00–320.00	7.73E+13	185.12	−0.99	0.03	
	70	260.00–320.00	1.65E+13	177.99	−0.99	0.04	
	90	260.00–320.00	2.96E+13	181.34	−0.99	0.03	
Beetroot	10	260.00–320.00	2.37E+06	102.94	−0.99	0.01	$[-\ln(1-a)]^3$
	30	280.00–340.00	3.17E+06	102.27	−0.99	0.01	
	50	290.00–350.00	8.07E+06	105.18	−0.99	0.02	
	70	290.00–350.00	1.10E+07	105.86	−0.99	0.02	
	90	300.00–360.00	2.55E+07	108.64	−0.99	0.02	

Table 4
Combustion kinetic parameters of switchgrass/bituminous coal at pre-peak.

Samples	β (°C/min)	t (°C)	A (s^{-1})	E_a (kJ/mol)	R	SD	$g(\alpha)$
20S80C	10	273.00–333.00	9.26E+12	209.73	−0.99	0.06	$[-\ln(1-a)]^4$
	30	293.00–353.00	3.16E+13	213.08	−0.99	0.04	
	50	302.00–362.00	2.53E+13	210.95	−0.99	0.05	
	70	308.00–368.00	4.74E+15	239.41	−0.99	0.07	
	90	305.00–365.00	1.33E+12	192.88	−0.99	0.05	
40S60C	10	266.00–326.00	4.97E+12	186.00	−0.99	0.06	$[-\ln(1-a)]^3$
	30	295.00–355.00	1.15E+12	181.31	−0.99	0.04	
	50	303.00–363.00	1.08E+12	181.28	−0.99	0.05	
	70	304.00–364.00	1.07E+13	190.99	−0.99	0.07	
	90	306.00–366.00	1.94E+08	139.09	−0.98	0.05	$\left[(1-a)^{-1/3}-1\right]^2$
60S40C	10	272.00–332.00	1.26E+08	135.51	−0.99	0.04	
	30	295.00–355.00	2.78E+08	139.01	−0.99	0.03	
	50	303.00–363.00	6.23E+08	142.18	−0.99	0.04	
	70	310.00–370.00	4.43E+08	143.11	−0.99	0.10	$\left[1-(1-a)^{1/3}\right]^{1/2}$
	90	313.00–373.00	8.65E+08	143.52	−0.99	0.06	$\left[(1-a)^{-1/3}-1\right]^2$
80S20C	10	274.00–334.00	1.82E+09	145.72	−0.99	0.06	
	30	287.00–347.00	1.23E+10	154.36	−0.99	0.03	
	50	298.00–358.00	1.62E+10	155.66	−0.99	0.04	
	70	307.00–367.00	8.05E+09	152.60	−0.99	0.05	
	90	306.00–366.00	5.06E+09	149.11	−0.99	0.04	
Switchgrass	10	269.00–329.00	7.69E+15	211.24	−0.99	0.09	$[-\ln(1-a)]^3$
	30	286.00–346.00	8.08E+16	223.64	−0.99	0.05	
	50	297.00–357.00	1.13E+11	163.70	−0.99	0.03	$\left[(1-a)^{-1/3}-1\right]^2$
	70	309.00–369.00	2.60E+11	167.87	−0.99	0.04	
	90	306.00–366.00	7.56E+10	160.68	−0.99	0.03	

Table 5
Combustion kinetic parameters of beetroot/bituminous coal at post-peak.

Samples	β (°C/min)	t (°C)	A (s^{-1})	E_a (kJ/mol)	R	SD	g(α)
Bituminous coal	10	480.00–530.00	7.17E+07	127.36	−0.99	0.01	$-\left[1-(1-a)^{-0.2}\right]/0.2$
	30	515.00–575.00	1.63E+02	56.51	−0.99	0.01	$\left[1-(1-a)^{0.2}\right]/0.2$
	50	546.00–596.00	7.97E+01	54.20	−0.99	0.01	$-\left[1-(1-a)^{-0.2}\right]/0.2$
	70	546.00–606.00	7.97E+01	54.20	−0.99	0.01	$-[1-(1-a)^{-0.2}]/0.2$
	90	574.00–624.00	1.11E+01	43.96	−0.99	0.01	$-[1-(1-a)^{-0.2}]/0.2$
20B80C	10	340.00–400.00	9.86E+04	119.22	−0.99	0.02	$[-\ln(1-a)]^4$
	30	350.00–410.00	5.64E+02	90.65	−0.99	0.02	
	50	350.00–410.00	1.40E+02	83.52	−0.99	0.04	
	70	350.00–410.00	1.01E+02	80.93	−0.99	0.04	
	90	340.00–400.00	1.03E+03	87.09	−0.99	0.08	
40B60C	10	320.00–380.00	7.58E+03	94.55	−0.99	0.07	
	30	340.00–400.00	3.74E+02	77.29	−0.99	0.07	
	50	340.00–400.00	5.19E+02	77.37	−0.99	0.09	
	70	350.00–410.00	8.29E+01	65.73	−0.98	0.09	
	90	340.00–420.00	2.52E+01	55.66	−0.98	0.07	
60B40C	10	320.00–380.00	1.44E+04	88.99	−0.99	0.11	
	30	340.00–400.00	1.74E+03	75.82	−0.98	0.11	
	50	340.00–420.00	2.26E+01	51.29	−0.99	0.05	
	70	350.00–430.00	6.56E+00	43.64	−0.99	0.03	
	90	340.00–420.00	1.25E+01	45.55	−0.98	0.05	
80B20C	10	320.00–380.00	3.73E+04	89.27	−0.98	0.13	
	30	300.00–360.00	1.41E+08	126.30	−0.99	0.01	$[-\ln(1-a)]^3$
	50	320.00–380.00	1.24E+08	125.08	−0.99	0.06	
	70	320.00–380.00	1.31E+08	124.03	−0.99	0.02	
	90	320.00–380.00	2.31E+08	127.15	−0.99	0.01	
Beetroot	10	320.00–400.00	3.88E+01	50.09	−0.99	0.01	$[-\ln(1-a)]^4$
	30	340.00–430.00	2.03E+01	43.38	−0.99	0.02	
	50	350.00–430.00	3.00E+01	43.11	−0.99	0.04	
	70	350.00–420.00	1.44E+01	38.06	−0.99	0.03	
	90	360.00–440.00	4.78E+01	41.8	−0.98	0.04	

Table 6
Combustion kinetic parameters of switchgrass/bituminous coal at post-peak.

Samples	β (°C/min)	t (°C)	A (s^{-1})	E_a (kJ/mol)	R	SD	g(α)
20S80C	10	333.00–393.00	2.20E+06	133.33	−0.99	0.13	$[-\ln(1-a)]^4$
	30	353.00–413.00	5.78E+04	110.52	−0.98	0.13	
	50	362.00–432.00	4.02E+02	82.37	−0.99	0.06	
	70	368.00–438.00	3.76E+02	82.06	−0.99	0.08	
	90	365.00–445.00	6.66E+01	69.21	−0.99	0.05	
40S60C	10	326.00–396.00	5.91E+03	88.82	−0.99	0.09	
	30	355.00–425.00	4.04E+02	75.92	−0.99	0.03	
	50	363.00–433.00	1.45E+02	69.81	−0.99	0.06	
	70	364.00–444.00	2.80E+01	58.15	−0.99	0.04	
	90	366.00–456.00	6.41E+00	48.14	−0.99	0.02	
60S40C	10	332.00–402.00	9.95E+02	72.32	−0.99	0.05	
	30	355.00–425.00	5.41E+02	67.66	−0.99	0.04	
	50	363.00–433.00	4.83E+02	64.84	−0.98	0.07	
	70	370.00–450.00	2.13E+01	50.12	−0.99	0.02	
	90	373.00–453.00	2.37E+01	50.12	−0.99	0.04	
80S20C	10	334.00–404.00	2.07E+03	70.46	−0.99	0.05	
	30	347.00–427.00	8.99E+03	73.98	−0.99	0.03	
	50	358.00–438.00	1.20E+03	63.18	−0.99	0.04	
	70	367.00–447.00	2.03E+02	54.04	−0.99	0.04	
	90	366.00–456.00	6.00E+01	45.86	−0.99	0.03	
Switchgrass	10	329.00–409.00	5.40E+03	71.36	−0.99	0.03	
	30	346.00–426.00	6.96E+04	81.32	−0.99	0.03	
	50	357.00–447.00	9.68E+03	69.37	−0.99	0.03	
	70	369.00–449.00	1.51E+03	58.86	−0.99	0.03	
	90	366.00–456.00	1.15E+03	55.64	−0.99	0.02	

in the reactant, usually at a surface and possibly at an imperfection. The initially generated germ nucleus, consisting of a few atoms only is generally regarded as unstable due to the high ratio of surface strain to volume. It may, however, develop into a growth nucleus, which increases in size through advance of the reactant-product interface into the bulk of the crystallite, so reducing the relative

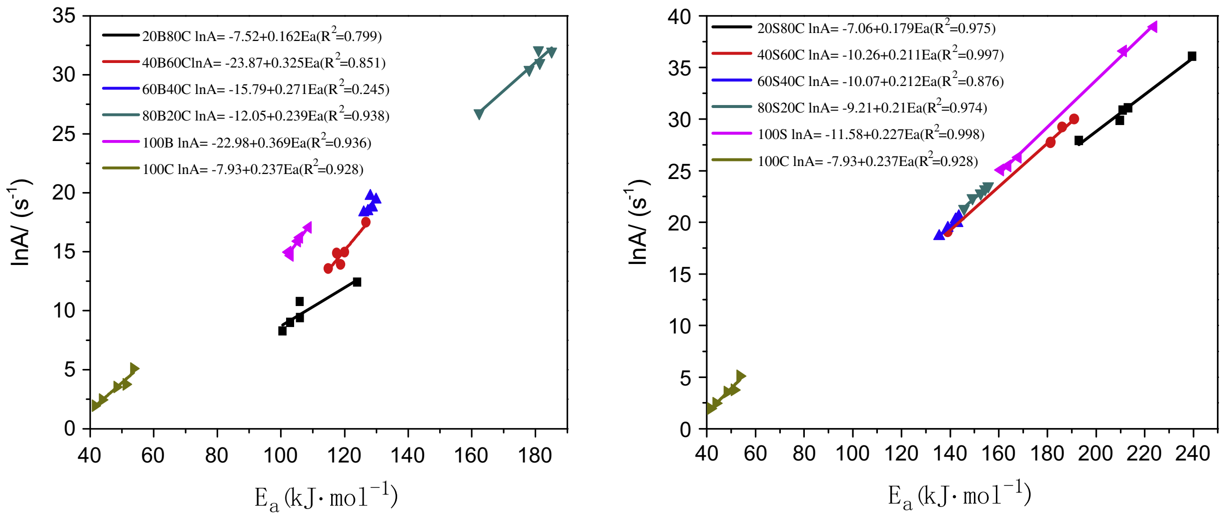

(a) Pre-peak period

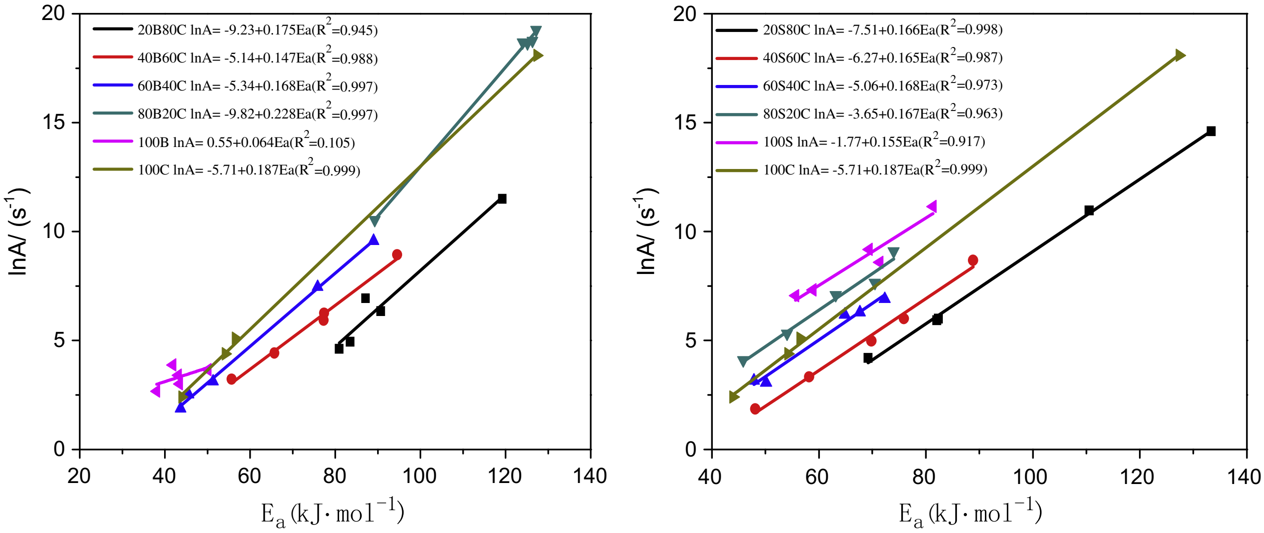

(b) Post-peak period

Fig. 4. Kinetic compensation effect of co-combustion of biomass and bituminous coal.

importance of the surface strain term. Therefore, the real activation energy and pre-exponential factor of the blend are gained, 118.76 kJ/mol and 1.12×10^6 s^{-1}. The best correlations for two stages are obtained with the activation energy and reaction mechanisms of all samples, as shown in Tables 3–6. The high correlation coefficient *R* values and low *SD* values indicate that the corresponding reaction model satisfactorily fits the experimental data.

From the tables, the dominant mechanisms associated with combustion kinetics for beetroot and beetroot/coal blends at pre-peak and post-peak are described by the Avrami–Erofeev equations ($n = 3$ or $n = 4$), which are controlled by the random nuclear producing and growing process. The mechanisms of combustion for switchgrass and switchgrass/coal blends at pre-peak are best fitted by the Avrami–Erofeev equation, Z–L–T equation or Anti-Jander equation (three dimensional diffusion); whereas their mechanisms are described by the Avrami–Erofeev equation ($n = 4$) at post-peak. Diffusion-controlled solid-state reaction kinetics in a sphere, where diffusion in all three directions is all-important. In a diffusion-controlled reaction, numerous chemical reactions or micro-structural changes in solids take place through solid-state diffusion, i.e. the movement and transport of gas molecules in the solid phase [36].

However, the mechanisms of combustion for blends are much different that of bituminous coal, which chemical reactions with different orders ($n = 0.2$, 0.5, 1, 1.5 for pre-peak; $n = 0.8$, 1.2 for post-peak) are presented. The chemical reaction order model implies that the rate-determining step is the chemical reaction which can be described by simple reaction order. The activation energies of co-combustion for beetroot and coal during the pre-peak period and post-peak period range from 100.53 to 185.12 kJ/mol, and from 43.64 to 127.15 kJ/mol, respectively. While for switchgrass/coal blends, their activation energies at pre-peak and post-peak range from 135.51 to 239.41 kJ/mol, and 45.86 to 133.33 kJ/mol, respectively. The relatively high activation energies may reflect to some extent dependence of pore structure on temperature. This implies that for the burning stage, higher temperature is required to provide the forward burning reaction. In general, reactions with higher activation energies are more temperature-sensitive [3]. Activation energies of combustion for poplar wood, and rice husk were calculated using three different isoconversional methods, Flynn–Wall–Ozawa, Kissinger, and ASTM I-II [28]. Quang-Vu et al. revealed that the combustion activation energy of hemicellulose varied from 103.8 to 44.8 kJ/mol for the spruce wood, and from 144.7 to 41.3 kJ/mol for the birch wood at a 10 °C/min heating rate based on the differential method [35]. That of char was from 183.1 to 109.4 kJ/mol for the spruce and from 222.0 to 132.3 kJ/mol for the birch. The activation energy of the cellulose was from 221.5 to 239.0 kJ/mol for the spruce, and from 204.7 to 236.7 kJ/mol for the birch. Oyedun et al. [37] obtained the pyrolysis activation energy of plastics and biomass blends at only a 10 °C/min heating rate based on the Coats–Redfern method. Combustion activation energy of microalgae in two stages at a 10 °C/min heating rate also based on the Coats–Redfern method was from 63 to 81 kJ/mol and from 113 to 126 kJ/mol, respectively [38]. Gil et al. [6] evaluated the combustion kinetics of bituminous coal, pine sawdust and their blends at a 15 °C/min heating rate based on the Coats–Redfern method. In the above literatures, only a single heating rate and several mechanism functions were considered. These models although based on experimental data apparently not impugned by heat and mass transfer effects, are not truly valid over widely variable conditions [13].

The kinetics characteristics of mixture samples had no linear relation with blend ratios due to interactions between biomass and coal.

The biomass ratios and heating ratios have no effect on mechanisms of beetroot/coal blends at pre-peak and post-peak, and switchgrass/coal blends at post-peak, but they have certain effect on the mechanisms of switchgrass/coal blends at pre-peak. According to the analysis principle of variance [39], the blending ratios have significant influence ($P < 0.05$) on the apparent activation energy of co-combustion for beetroot/coal and switchgrass/coal blends at pre-peak and at post-peak, while the heating rates have more significant influence ($P < 0.05$, higher F value) on the apparent activation energy of co-combustion for switchgrass/coal blends at post-peak than blending ratios.

3.3. Compensation effects

Moreover, by analyzing the data in above tables, a linear relation between E_a and $\ln A$ of each sample is revealed within heating rate of 10 °C/min to 90 °C/min. Fig. 4 summarizes the results. There are much less correlation coefficients for 60B40C blend at pre-peak and pure beetroot at post-peak, because their activation energies have not obvious change with different heating rates.

Both the pre-exponential factor and the activation energy increases or decreases with the variation of heating rate, so the two parameters can compensate their effect on the co-combustion rate according to the Arrhenius principle [40]. The increase of the pre-exponential factor seems to attenuate the decrease of reaction rate constant caused by increase of the apparent activation energy with the variation of heating rate. Compensation effect makes it more complicated for co-combustion of coal and biomass in different heating rates, because the decrease of the apparent activation energy and the pre-exponential factor play opposite roles on combustion rate. The kinetics compensation effects are also discovered in biomass pyrolysis, and pyrolysis and combustion characteristics of coal chars, respectively [41,42]. A marked compensation effect is presented for the gasification reaction of biomass residues [43].

4. Conclusions

The beetroot and beetroot/coal blends showed 3–4 peaks for combustion of volatiles and fixed carbon. The blending ratios had significant effect on the apparent activation energy of co-combustion for beetroot/bituminous coal or switchgrass/bituminous coal. The heating rates have more significant influence on the apparent activation energy of co-combustion for switchgrass/coal blends at post-peak. The activation energies of co-combustion for beetroot and coal during the pre-peak period and post-peak period ranged from 100.53 to 185.12 kJ/mol, and from 43.64 to 127.15 kJ/mol, respectively. While for switchgrass/coal blends, their activation energies at pre-peak and post-peak ranged from 135.51 to 239.41 kJ/mol, and 45.86 to 133.33 kJ/mol, respectively. A linear relationship between $\ln A$ and E_a provides a way to predict the kinetic parameters.

Acknowledgment

This work was supported by the National Natural Science Foundation of China under No. 51376017.

Appendix A. Supplementary material

Supplementary data associated with this article can be found, in the online version, at http://dx.doi.org/10.1016/j.fuel.2014.11.085.

References

[1] Vamvuka D, Sfakiotakis S. Combustion behaviour of biomass fuels and their blends with lignite. Thermochim Acta 2011;526:192–9.
[2] Hansson J, Berndes G, Johnsson F, Kjärstad J. Co-firing biomass with coal for electricity generation-An assessment of the potential in EU27. Energy Policy 2009;37:1444–55.
[3] Masnadi MS, Habibi R, Kopyscinski J, Hill JM, Bi X, Lim CJ, et al. Fuel characterization and co-pyrolysis kinetics of biomass and fossil fuels. Fuel 2014;117(Part B):1204–14.
[4] Ogden CA, Ileleji KE, Johnson KD, Wang Q. In-field direct combustion fuel property changes of switchgrass harvested from summer to fall. Fuel Process Technol 2010;91:266–71.
[5] Rezaei F, vander Gheynst JS. Critical moisture content for microbial growth in dried food-processing residues. J Sci Food Agric 2010;90:2000–5.
[6] Gil MV, Casal D, Pevida C, Pis JJ, Rubiera F. Thermal behaviour and kinetics of coal/biomass blends during co-combustion. Bioresour Technol 2010;101:5601–8.
[7] Darvell LI, Jones JM, Gudka B, Baxter XC, Saddawi A, Williams A, et al. Combustion properties of some power station biomass fuels. Fuel 2010;89:2881–90.
[8] Aho M, Gil A, Taipale R, Vainikka P, Vesala H. A pilot-scale fireside deposit study of co-firing Cynara with two coals in a fluidised bed. Fuel 2008;87:58–69.
[9] Di Nola G, de Jong W, Spliethoff H. TG-FTIR characterization of coal and biomass single fuels and blends under slow heating rate conditions: Partitioning of the fuel-bound nitrogen. Fuel Process Technol 2010;91:103–15.
[10] Kubacki ML, Ross AB, Jones JM, Williams A. Small-scale co-utilisation of coal and biomass. Fuel 2012;101:84–9.
[11] Muthuraman M, Namioka T, Yoshikawa K. A comparison of co-combustion characteristics of coal with wood and hydrothermally treated municipal solid waste. Bioresour Technol 2010;101:2477–82.
[12] Haykiri-Acma H, Yaman S. Effect of co-combustion on the burnout of lignite/biomass blends: a Turkish case study. Waste Manage (Oxford) 2008;28:2077–84.
[13] Branca C, Di Blasi C. A unified mechanism of the combustion reactions of lignocellulosic fuels. Thermochim Acta 2013;565:58–64.
[14] Gharebaghi M, Irons RM, Pourkashanian M, Williams A. An investigation into a carbon burnout kinetic model for oxy-coal combustion. Fuel Process Technol 2011;92:2455–64.
[15] Lai Z, Ma X, Tang Y, Lin H, Chen Y. Thermogravimetric analyses of combustion of lignocellulosic materials in N_2/O_2 and CO_2/O_2 atmospheres. Bioresour Technol 2012;107:444–50.
[16] Zhaosheng Y, Xiaoqian M, Ao L. Thermogravimetric analysis of rice and wheat straw catalytic combustion in air- and oxygen-enriched atmospheres. Energy Convers Manage 2009;50:561–6.
[17] Bamford CH, Tipper CFH. Comprehensive chemical kinetics. Amsterdam, The Netherlands: Elsevier Scientific Publishing Company; 1980.
[18] Liu X, Chen M, Yu D. Oxygen enriched co-combustion characteristics of herbaceous biomass and bituminous coal. Thermochim Acta 2013;569:17–24.
[19] Liu X, Chen MQ, Yu D, Lu TJ. Analysis of influence factors on co-combustion characteristics of bituminous coal with herbal biomass. Trans Chin. Soc Agric Eng 2012;28:200–7.
[20] Luo X, Wang L, Zhao X, Xu G, Wu H. Experimental investigation of heat transfer in a rotor–stator cavity with cooling air inlet at low radius. Int J Heat Mass Transfer 2014;76:65–80.
[21] Abbassi Y, Talebi M, Shirani AS, Khorsandi J. Experimental investigation of TiO_2/water nanofluid effects on heat transfer characteristics of a vertical annulus with non-uniform heat flux in non-radiation environment. Ann Nucl Energy 2014;69:7–13.
[22] Fornasini P. The uncertainty in physical measurements – an introduction to data analysis in the physics laboratory. New York: Springer; 2008.

[23] Li X, Li H, Liu H, Zhu G. Non-isothermal thermal decomposition reaction kinetics of dimethylhexane-1,6-dicarbamate (HDC). J Hazard Mater 2011;198:376–80.
[24] Pourmortazavi SM, Kohsari I, Teimouri MB, Hajimirsadeghi SS. Thermal behaviour kinetic study of dihydroglyoxime and dichloroglyoxime. Mater Lett 2007;61:4670–3.
[25] Barral L, Diez FJ, Garcia-Garabal S, Lopez J, Montero B, Montes R, et al. Thermodegradation kinetics of a hybrid inorganic–organic epoxy system. Eur Polym J 2005;41:1662–6.
[26] Zhang Z, Liang G, Ren P, Wang J. Thermodegradation kinetics of epoxy/DDS/POSS system. Polym Compos 2007;28:755–61.
[27] Bianchi O, Oliveira RVB, Fiorio R, Martins JDN, Zattera AJ, Canto LB. Assessment of Avrami, Ozawa and Avrami–Ozawa equations for determination of EVA crosslinking kinetics from DSC measurements. Polym Test 2008;27:722–9.
[28] Kok MV, Özgür E. Thermal analysis and kinetics of biomass samples. Fuel Process Technol 2013;106:739–43.
[29] Vlaev LT, Markovska IG, Lyubchev LA. Non-isothermal kinetics of pyrolysis of rice husk. Thermochim Acta 2003;406:1–7.
[30] Biswas S, Mohanty P, Sharma DK. Studies on synergism in the cracking and co-cracking of Jatropha oil, vacuum residue and high density polyethylene: kinetic analysis. Fuel Process Technol 2013;106:673–83.
[31] Vyazovkin S, Wight CA. Model-free and model-fitting approaches to kinetic analysis of isothermal and nonisothermal data. Thermochim Acta 1999;340–341:53–68.
[32] Hu R, Gao S, Zhao F, Shi Q, Zhang T, Zhang J. Kinetics of thermal analysis. Beijing, China: Science Press; 2008.
[33] Prins MJ, Ptasinski KJ, Janssen F. Torrefaction of wood – Part 1. Weight loss kinetics. J Anal Appl Pyrol 2006;77:28–34.
[34] Singh S, Kumar S. New approach for thermal testing of solar dryer: development of generalized drying characteristic curve. Sol Energy 2012;86:1981–91.
[35] Bach Q-V, Tran K-Q, Skreiberg Ø, Khalil RA, Phan AN. Effects of wet torrefaction on reactivity and kinetics of wood under air combustion conditions. Fuel 2014;137:375–83.
[36] Yorulmaz SY, Atimtay AT. Investigation of combustion kinetics of treated and untreated waste wood samples with thermogravimetric analysis. Fuel Process Technol 2009;90:939–46.
[37] Oyedun AO, Tee CZ, Hanson S, Hui CW. Thermogravimetric analysis of the pyrolysis characteristics and kinetics of plastics and biomass blends. Fuel Process Technol 2014;128:471–81.
[38] López-González D, Fernandez-Lopez M, Valverde JL, Sanchez-Silva L. Kinetic analysis and thermal characterization of the microalgae combustion process by thermal analysis coupled to mass spectrometry. Appl Energy 2014;114:227–37.
[39] Moore DS, McCabe GP, Craig BA. Introduction to the practice of statistics. 6th ed. New York: W.H. Freeman and Company; 2009.
[40] Chen MQ, Chen YX, Jia L, Zhang YG, Li QH, Meng AH. Kinetic analysis on the drying of high moisture MSW. Heat Transfer – Asian Res 2009;38:216–22.
[41] White JE, Catallo WJ, Legendre BL. Biomass pyrolysis kinetics: a comparative critical review with relevant agricultural residue case studies. J Anal Appl Pyrol 2011;91:1–33.
[42] Wang Ca, Zhang X, Liu Y, Che D. Pyrolysis and combustion characteristics of coals in oxyfuel combustion. Appl Energy 2012;97:264–73.
[43] Wu YQ, Wu SY, Li Y, Gao JS. CO_2 gasification characteristics of biomass residues from agricultural and woody production. Energy Sources, Part A: Recovery, Utilization Environ Effects 2013;35:574–84.